BRAIN COMMUNICATIONS

The subcortical default mode network and Alzheimer's disease: a systematic review and meta-analysis

Sara Seoane,[1,2,3] Martijn van den Heuvel,[1,4] Ángel Acebes[2,5] and Niels Janssen[2,3,6]

The default mode network is a central cortical brain network suggested to play a major role in several disorders and to be particularly vulnerable to the neuropathological hallmarks of Alzheimer's disease. Subcortical involvement in the default mode network and its alteration in Alzheimer's disease remains largely unknown. We performed a systematic review, meta-analysis and empirical validation of the subcortical default mode network in healthy adults, combined with a systematic review, meta-analysis and network analysis of the involvement of subcortical default mode areas in Alzheimer's disease. Our results show that, besides the well-known cortical default mode network brain regions, the default mode network consistently includes subcortical regions, namely the thalamus, lobule and vermis IX and right Crus I/II of the cerebellum and the amygdala. Network analysis also suggests the involvement of the caudate nucleus. In Alzheimer's disease, we observed a left-lateralized cluster of decrease in functional connectivity which covered the medial temporal lobe and amygdala and showed overlap with the default mode network in a portion covering parts of the left anterior hippocampus and left amygdala. We also found an increase in functional connectivity in the right anterior insula. These results confirm the consistency of subcortical contributions to the default mode network in healthy adults and highlight the relevance of the subcortical default mode network alteration in Alzheimer's disease.

1 Department of Complex Traits Genetics, Center for Neurogenomics and Cognitive Research (CNCR), Amsterdam Neuroscience, Vrije Universiteit Amsterdam, Amsterdam 1081 HV, The Netherlands
2 Institute of Biomedical Technologies (ITB), University of La Laguna, Tenerife 38200, Spain
3 Instituto Universitario de Neurociencia (IUNE), University of La Laguna, Tenerife 38200, Spain
4 Department of Child and Adolescent Psychiatry and Psychology, Section Complex Trait Genetics, Amsterdam Neuroscience, Vrije Universiteit Medical Center, Amsterdam UMC, Amsterdam 1081 HV, The Netherlands
5 Department of Basic Medical Sciences, University of La Laguna, Tenerife 38200, Spain
6 Department of Cognitive, Social and Organizational Psychology, University of La Laguna, Tenerife 38200, Spain

Correspondence to: Sara L. Seoane
Department of Complex Trait Genetics
Center for Neurogenomics and Cognitive Research (CNCR)
Vrije Universiteit Amsterdam, De Boelelaan 1085, Amsterdam 1081 HV,
The Netherlands
E-mail: saralseoane@gmail.com

Keywords: default mode network; subcortical; functional connectivity; Alzheimer's disease

Received October 09, 2023. Revised February 28, 2024. Accepted April 09, 2024. Advance access publication April 10, 2024

Graphical Abstract

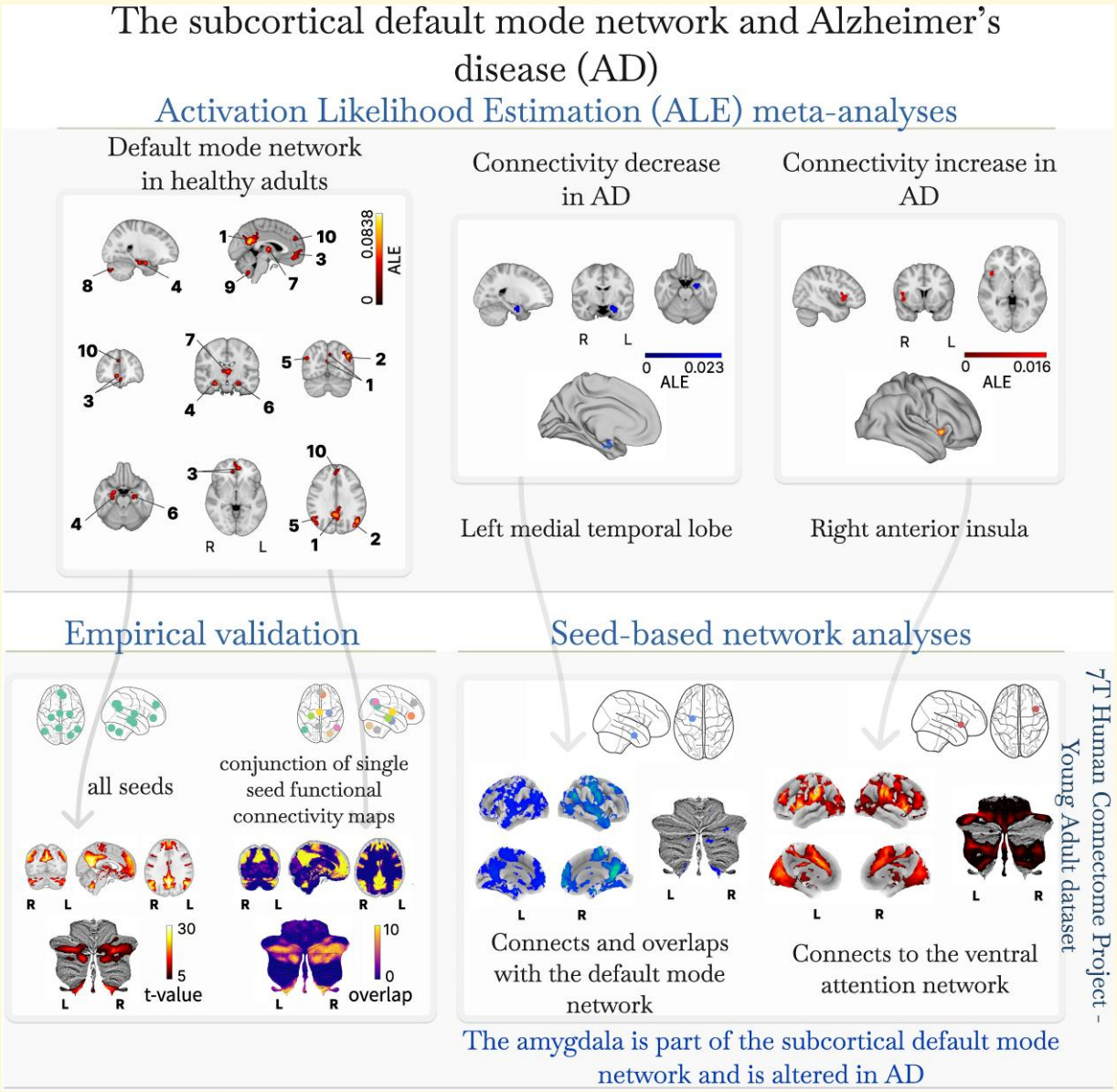

Introduction

Our understanding of the default mode network emerged from the observation of a characteristic brain spatial pattern of increased blood flow during resting wakefulness and decreased blood flow during externally oriented tasks.[1,2] The default mode network is considered the most prevalent brain pattern of coactivation during resting state[3-7]; a network crucially implicated in mental and neurological disorders such as schizophrenia,[8] multiple sclerosis[9] and Alzheimer's disease[10,11]; and a suggested target for interventions and biomarkers in Alzheimer's disease.[12,13] Our understanding of its cortical components has greatly advanced.[14-18] However, the study of the subcortical components of the network and their alterations, particularly in the context of Alzheimer's disease, has not yet derived a clear list of subcortical structures. This study investigates the subcortical regions within the default mode network and their functional connectivity alterations in Alzheimer's disease.

Previous studies identified subcortical brain regions within the default mode network.[19-22] Among the early studies into resting-state brain blood flow spatial patterns, the amygdala and the cerebellum were identified as components of what is now recognized as the default mode network.[2,23] An increasing number of recent studies find subcortical regions with functional and anatomical connections to the default mode network, including the amygdala, anterior and mediodorsal thalamus, basal forebrain, nucleus accumbens,

Table 1 Summary of Population, Intervention, Comparator, and Outcome (PICO) components per question

	Default mode network in healthy participants	FC alterations and their directions in Alzheimer's disease
Population	Healthy participants	Patients that meet the criteria for possible or probable Alzheimer's disease
Intervention	FC analysis of the default mode network or its seeds performed on whole-brain data	Comparison of whole-brain FC between Alzheimer's disease and matched HC groups (Alzheimer's disease > HC and Alzheimer's disease < HC)
Comparator	None needed	Healthy elderly controls
Outcome	What are the cortical and subcortical nodes of the default mode network?	What are the brain sites of increases and decreases in FC in Alzheimer's disease? How do they relate to the default mode network?

HC, healthy controls; FC, functional connectivity.

medial septal nucleus, ventral tegmental area, dorsal raphe nucleus, dopaminergic nuclei of the brainstem, caudate nucleus, hypothalamus and cerebellum.[3,21,24-31] Several of these subcortical structures, such as the basal forebrain, the brainstem, amygdala and thalamus, are not just part of the network but actively modulate the activity of the default mode network and its interplay with other large-scale networks.[26,27,32]

Given the known impact of Alzheimer's disease on subcortical structures[33-37] and the default mode network,[11,37,38] it is crucial to identify the subcortical regions of the default mode network that are altered in Alzheimer's disease. The earliest signs of Alzheimer's disease pathology manifest as tau aggregations in the locus coeruleus, even in individuals as young as 10–20 years old.[33] This alteration progressively impacts other subcortical regions, the medial temporal lobe and, eventually, cortical regions linked to the default mode network.[33,39] The spreading of amyloid-beta aggregation concurrently progresses from cortical default mode network regions[40] to regions of the medial temporal lobe and subcortical regions.[33,39,41] Despite the unclear progression sequence, early stages of the disease significantly affect various subcortical brain regions, including the brainstem, cerebellum, limbic and anterior thalamus, caudate nucleus, putamen and amygdala.[34,42-46]

Functional connectivity of the default mode network and subcortical regions is altered in Alzheimer's disease and tightly linked to protein pathology.[39,40,47] Previous studies have predominantly observed decreased functional connectivity in the default mode network[47,48] and variable changes in its subnetworks.[49,50] The hippocampus displays both increased and decreased functional connectivity with brain regions including the default mode network.[51-53] The amygdala, the thalamus and Crus II and lobule IX of the cerebellum show reduced functional connectivity with default mode network regions.[35,36,54] Notably, these regions also exhibit hallmark Alzheimer's disease pathology.[40,44,45,47,55] A recently proposed model describes the intertwined relationship between these alterations in two regions of the default mode network: the medial temporal lobe and the posteromedial cortex.[39] This interplay leads to a cycle of atrophy, hyperexcitability and further tau pathology accumulation, particularly impacting regions within the medial temporal lobe, an area particularly vulnerable in Alzheimer's disease.[39,44,56] Therefore, characterizing the functional connectivity alterations within the network could be crucial for identifying treatment targets.

Regardless of numerous advances in the field, our understanding of the subcortical components of the default mode network, as well as of the subcortical default mode network alterations in Alzheimer's disease, remains incomplete. The lack of consistent results may be linked to at least three main reasons. First, a branch of neuroimaging analysis methods based on the projection of the cortical data from a volume to a surface has improved our cortical spatial precision.[57] However, this often results in the neglect of subcortical regions and the hippocampus, unless used in combination with volume-based methods.[58] Second, the signal-to-noise ratio in magnetic resonance images is notably lower in some areas of the brain, including subcortical structures.[59,60] Given that the detection of functional connectivity between brain regions is influenced by the quality of the signals,[24] the regional difference in signal quality could impact our ability to detect functional connectivity. Third, subcortical structures are small and variable, which makes it difficult to align them for group analysis.[20] Thus, conducting a systematic study of the findings of subcortical default mode network components and their alterations in Alzheimer's disease is a crucial task not yet done, key to identifying the most consistent regions across studies.

In this study, we performed a systematic review, meta-analysis and empirical validation of cortical and subcortical default mode network regions in healthy individuals. We also conducted a systematic review, meta-analysis, seed-based network analysis and conjunction analysis of the cortical and subcortical brain sites that present functional connectivity alterations in Alzheimer's disease and their connectivity with default mode network regions (see Table 1). We reduced bias in examining the subcortical default mode network alterations in Alzheimer's disease by meta-analysing the brain sites that show altered functional connectivity to any brain region in the disease and then determining whether these brain sites were part of the default mode network in healthy normal conditions. We expected to find subcortical structures of the default mode network including the thalamus, caudate nucleus, amygdala, Crus I/II and lobule IX of the cerebellum, brainstem and basal forebrain. Another anticipation was to identify brain cortical and subcortical sites of decreased functional connectivity in Alzheimer's disease that included the precuneus, hippocampus, thalamus, brainstem and cerebellum. Identifying the consistent involvement of subcortical structures in the

default mode network, the changes in functional connectivity in Alzheimer's disease as well as the link between the brain sites of alteration and networks has the potential to impact our knowledge of the network's role in the disease.

Materials and methods

Search strategy and database selection

This study follows the Preferred Reporting Items for Systematic Reviews and Meta-Analyses (PRISMA) guidelines[61] and uses PubMed, Scopus, Web of Science (WoS) and NeuroVault[62] for database searches. The search was conducted between 4 May 2022 and 1 June 2022 and included the 'All Fields' option in PubMed; title, abstract and keywords in Scopus; and title, abstract, keywords and automatically generated terms from the titles of the cited papers in WoS. We did not limit our search to a specific timeframe. The search details, including queries, search dates and number of results are documented in Supplementary Tables 1 and 2. We also scrutinized the reference sections and the studies previously known to the authors for complete coverage (see Fig. 1).

Selection criteria

Study search and selection were performed by S.S. and revised by N.J. For the healthy adult default mode network meta-analysis, whole-brain studies that examined the intrinsic functional connectivity of the default mode network in healthy adults (18–55 years old) and which reported results in standard anatomical space (Montreal Neurological Institute, MNI, or Talairach) were included. To include as many articles for the meta-analysis as possible while excluding articles with extremely small sample sizes, we selected studies with at least 15 participants. Only studies that examined whole-brain functional MRI (fMRI) data (using volume-based or combined surface- and volume-based methods) were considered. This excluded, for example, studies that only included cortical regions in their analysis. Coordinates reported in the manuscripts as part of the default mode network or connected to its most central brain regions (i.e. the precuneus/posterior cingulate cortex/retrosplenial cortex) were included in the analysis. Negative functional connectivity or 'anticorrelations' were not considered for the analysis. Resting-state fMRI studies were considered for inclusion, regardless of whether they had closed or open eyes and whether there was a visual fixation.

For the Alzheimer's disease coactivation alteration meta-analysis, included studies were case-control studies that examined whole-brain functional connectivity differences between Alzheimer's disease (AD) patients and healthy controls (HC). Only records in which the patients met the criteria for possible or probable Alzheimer's disease published by the National Institute of Neurological and Communicative Diseases and Stroke/Alzheimer's Disease and Related Disorders Association (NINCDS-ADRDA) or the National Institute on Aging—Alzheimer's Association (NIA-AA) were included. All included studies had at least 10 participants in both patients and control groups. We used a lower sample size threshold taking into account that samples in case-control studies tend to be low. All experiments from the selected articles that consisted of Alzheimer's disease > HC or Alzheimer's disease < HC contrasts were included. Finally, the quality of the studies included in the meta-analysis of Alzheimer's disease brain sites was assessed using the Critical Appraisal Skills Programme (CASP[63]) checklist for case-control studies.

Data extraction

For the healthy adult default mode network meta-analysis, the extracted data included sample size, age, gender, network extraction technique and coordinate space in which the coordinates are provided in the study, presence of subcortical regions in the results and coordinates of the default mode network (see Supplementary Table 3). Variables extracted from the included studies in the Alzheimer's disease coactivation alteration meta-analysis were sample size, gender, age, diagnostic criteria for Alzheimer's disease, Clinical Dementia Rating (CDR) scores, Mini-Mental State Examination (MMSE) scores, Montreal Cognitive Assessment (MoCA) scores, years of education, biomarkers used, apolipoprotein E (APOE) alleles, main analysis technique used and coordinates for brain sites with altered functional connectivity in Alzheimer's disease compared with HC (see Supplementary Tables 4 and 5 and Supplementary Fig. 1).

The extracted data included sets of coordinates, or foci, in either MNI or Talairach space. These foci were extracted from the manuscripts, Supplementary Methods and openly available volumes. Each included article could have multiple functional connectivity maps for the default mode network or sets of functional connectivity alteration sites in Alzheimer's disease. Each functional connectivity or contrast map was treated as an independent experiment in the meta-analysis. See more in the Supplementary Methods section.

Statistical analysis

Meta-analysis procedure

Three meta-analyses of brain maps were performed: first, a meta-analysis using foci from experiments of the default mode network in healthy adults; second, a meta-analysis using foci with increased functional connectivity in Alzheimer's disease patients against HC (Alzheimer's disease > HC); and third, a meta-analysis of foci with decreased functional connectivity in Alzheimer's disease patients against HC (Alzheimer's disease < HC). Separate foci files were prepared for the three meta-analyses, and activation likelihood estimation (ALE) was calculated using the GingerALE software.[64,65] ALE meta-analysis is a coordinate- and kernel-based method for meta-analysis of neuroimaging data. This method consists of three main steps: first, the interpolation of a three-

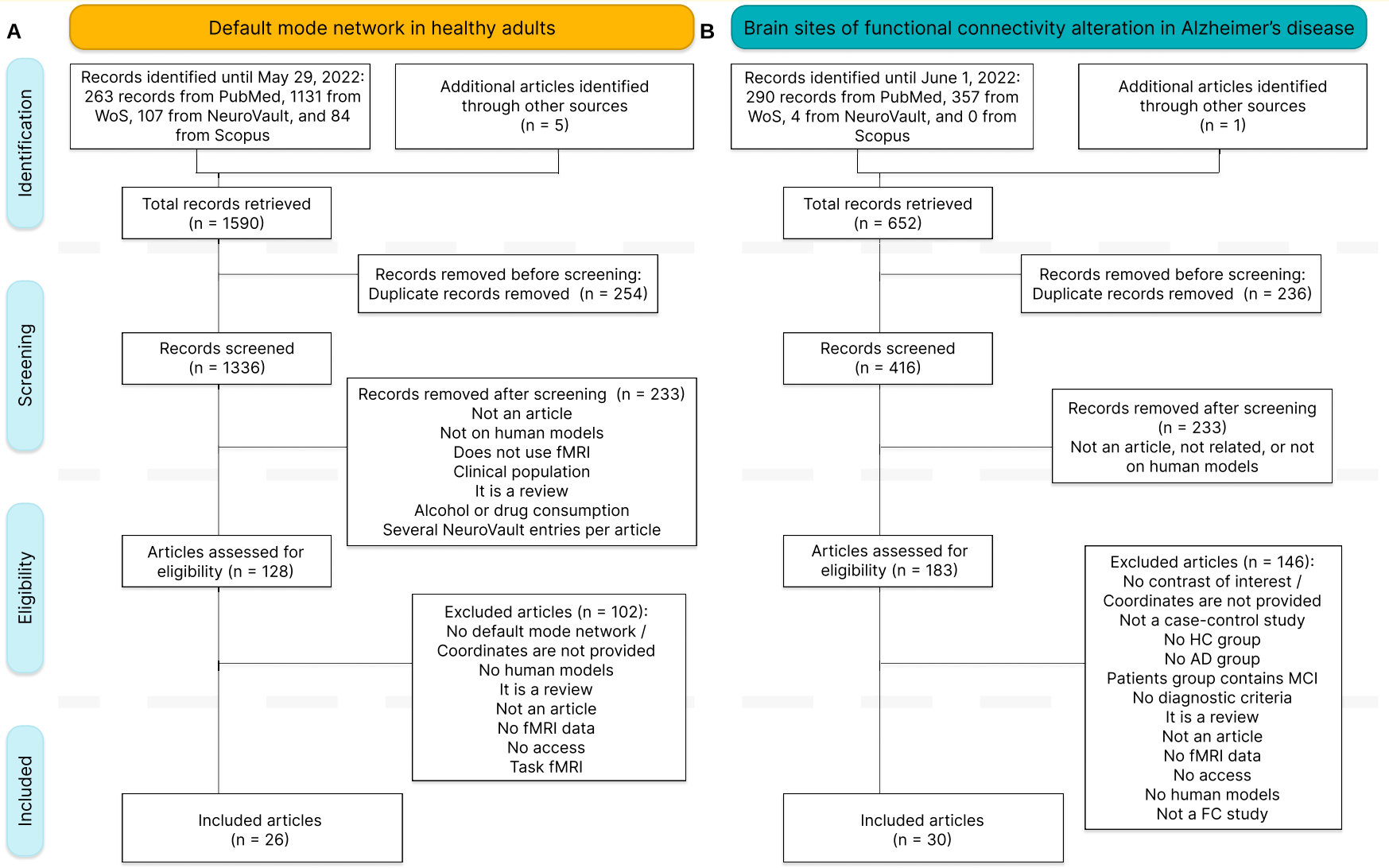

Figure 1 PRISMA workflows. Workflows for (**A**) the default mode network in healthy adults and for (**B**) functional connectivity alterations in Alzheimer's disease. The workflow is divided into four phases (from top to bottom): identification, screening, eligibility and inclusion. In the identification phase, the initial search retrieved 1586 records for question 1 and 652 records for question 2. These records were reduced in the screening and eligibility phases to 26 and 30 articles that were used in this meta-analysis.

dimensional Gaussian distribution (or kernel) around each focus (set of three coordinates): second, a combination of the resulting maps for each experiment; and third, the calculation, through a non-additive random effects model, of a single combined map that represents the consistent activations across experiments. This model uses the sample size per experiment, given its impact on statistical power, to find statistical effects. Moreover, the significance of this map is assessed by a Monte Carlo test under the null hypothesis of complete spatial randomness.[66-68] The three meta-analyses were performed using the default cluster-level family-wise estimation (FWE) correction at $P < 0.01$, 1000 permutations and thresholding of $P < 0.001$.

Data set used for empirical validation and network analysis

A resting-state fMRI sample was used in both the validation analysis of the default mode network brain regions and the network analysis from the altered brain sites in Alzheimer's disease. This data set consisted of resting-state fMRI data from 172 healthy young participants in the 7T WU-Minn Human Connectome Project's 1200 subjects' data set. These participants were between 22 and 35 years old, 60% female. Please find more information in the Supplementary Methods and elsewhere.[69] The data analyses were conducted in agreement with the declaration of Helsinki and with the protocol established by the Ethics Commission for Research of the Universidad de La Laguna, the Comité de Ética de la Investigación y Bienestar Animal.

Empirical validation of the cortical and subcortical default mode network

The brain regions identified in the healthy adult default mode network meta-analysis served as seeds to calculate new functional connectivity maps. Spherical regions of interest (ROIs) were created around the peak ALE MNI coordinates of the brain regions resulting from the meta-analysis of the default mode network in healthy adults using FSL's (FMRIB Software Library) `fslmaths`. Spheres had a radius of 4 mm each, and the average time series of the voxels inside each sphere was extracted for each subject and resting-state session using FSL's `fslmeants`. Each average time series was regressed to the individual whole-brain resting-state fMRI data in a general linear model with `fsl_glm` program. Group-level functional connectivity analysis was performed for each ROI using FSL's `randomise` and consisted of randomized non-parametric voxel-wise one-sample *t*-tests (5000 permutations), threshold-free cluster enhancement and $P < 0.001$ as the statistical threshold. A conjunction analysis of the group functional connectivity maps was performed using the Analysis of Functional NeuroImages's (AFNI) `3dcalc` function to determine the overlap between the functional connectivity maps of individual ROIs. An additional seed-based functional connectivity analysis was performed using the same procedure as with each individual ROI but regressing the average time series across the 10 seeds. The group-level map was also obtained using `randomise` with randomized non-parametric voxel-wise one-sample *t*-tests (5000 permutations), threshold-free cluster enhancement and $P < 0.001$ as the statistical threshold.

Network analysis of functional connectivity alterations in Alzheimer's disease

The connection between the meta-analytical brain sites of functional connectivity alteration in Alzheimer's disease and the default mode was assessed through a seed-based analysis following the same procedure as per the empirical validation of the default mode network brain regions, except that this time no conjunction analysis was performed across functional connectivity maps of alteration sites. We performed this analysis on the same sample of healthy young adults to identify the large-scale networks to which the altered brain sites belong under normal healthy conditions.

Results

Filtered search results

Systematic searches were performed separately for studies related to the default mode network in healthy adults and to the functional connectivity case-control studies in Alzheimer's disease. The 2 independent searches retrieved 1585 and 651 records, respectively. Six additional articles were identified and included in the lists, for a total of 1590, and 652 records. After the removal of duplicate records, a total of 1336 records remained from the default mode network in healthy adults searches and a total of 417 from the case-control studies searches. The first screening was performed to filter records that were not related to the questions, were not human model studies, did not use fMRI, studied clinical populations or were not scientific research articles. A total of 128 articles of the default mode network in healthy adults and 183 articles of the Alzheimer's disease functional connectivity differences were assessed for eligibility, and 26 and 30 studies were included in the meta-analyses (see Fig. 1).

For the healthy adult default mode network meta-analysis, a total of 852 foci from 55 experiments in 26 articles were used. The sample sizes ranged from 15 to 500 (median = 59), with weighted pooled proportion (pP) of 49% males and weighted pooled mean (pM) age of 29.28 years old (20.63–42.30 years old). The total sample size across all these experiments was 5165. See Supplementary Table 3 for a more detailed description of the sample.

The meta-analysis of the Alzheimer's disease < HC contrast included 40 experiments from 26 studies. For each experiment, we used the smallest sample size between case and control groups to weight the neuroimaging meta-analysis, leading to a total sample size of 927. The number of participants with Alzheimer's disease per experiment

ranged from 10 to 70 (median = 20.71; pP = 45% male), and the number of HC ranged from 10 to 174 (median = 32.88; pP = 44% male). Alzheimer's disease participants were 71.03 years old, and HC were 68.34 years old, on average. CDR scores were reported in 17 studies, with a CDR score 0 in HC and 0.9 (range of 0.5–1.3) in Alzheimer's disease. MMSE scores were reported in 20 studies, with a pM 28.82 for the HC group and 20.43 for the Alzheimer's disease group. HC had 12.43 years of education and Alzheimer's disease had 10.69. Data on additional cognitive tests (e.g. MoCA, AVLT) and biomarkers were reported in some studies, but the reports were either too variable or scarce to make a global summary. The predominant diagnosis among the included studies was probable Alzheimer's disease (17 studies, 12 being exclusively probable Alzheimer's disease), alongside reports of possible Alzheimer's disease, mild Alzheimer's disease and Alzheimer's disease. Six studies, based on McKhann *et al.*[70] criteria or unspecified NINCDS-ADRDA guidelines, might have included some patients with mild cognitive impairment, a point discussed in McKhann *et al.*[71] For detailed information per study, please see Supplementary Table 4 and Supplementary Fig. 1.

The meta-analysis of the Alzheimer's disease > HC contrast included 20 experiments from 15 studies. Sample sizes in the Alzheimer's disease group ranged from 10 to 70 (median = 19), with an average age of 73.69 years old, and 46% being male. Sample sizes in the HC groups ranged from 10 to 67 (median = 16.50), with an average age of 70.68 years old, 48% male. Considering the smallest group size for each case-control pair, the total sample size for the neuroimaging meta-analysis was 426. CDR scores were reported in 10 studies and were 0 for HC and 0.83 for Alzheimer's disease (range of 0.5–1.26). Thirteen studies reported MMSE scores, with a pM 28.66 for HC and 21.79 for Alzheimer's disease. Eleven studies provided data on the years of education, with 13.16 years in HC and 21.79 in Alzheimer's disease. Seven of the 15 studies reported probable Alzheimer's disease diagnosis, with one of them indicating possible or probable Alzheimer's disease diagnosis. See Supplementary Table 5 and Supplementary Fig. 1 for detailed information per study. The included studies did not report any specific subtypes of Alzheimer's disease.

Cortical and subcortical components of the default mode network

The healthy adult default mode network ALE meta-analysis resulted in 10 consistent clusters. These clusters covered the (extensively documented) cortical posterior and anterior cingulate cortices, precuneus, inferior parietal lobule, angular gyrus, medial frontal pole, ventromedial prefrontal cortex, anterior and middle parahippocampal gyrus and hippocampus. Regarding the main focus of this study, the clusters also covered the subcortical thalamus, amygdala and Crus I/II and lobule and vermis IX of the cerebellum (see Table 2 and Fig. 2). Contributions from cortical regions, thalamus and cerebellar lobule IX to the default mode network were bilateral, and cerebellar Crus I/II contributions were right-lateralized.

Brain sites of functional connectivity alterations in Alzheimer's disease

One cluster of functional connectivity decrease and another cluster of functional connectivity increase were found in Alzheimer's disease compared with controls (see Fig. 3). The brain site of decreased coactivation was 100% left-lateralized and covered the parahippocampal gyrus, amygdala and hippocampus. It had a maximum ALE value at −26, −8 and −26 MNI coordinates (ALE =

Table 2 Clusters coverage in the resting-state default mode network in healthy adults

Cluster number	Brain regions covered	Lateralization	Coordinates in MNI152 space (peak ALE value)	ALE	*P*-value	z-value
1	Posterior cingulate gyrus, precuneus	Bilateral (65.2% L; 34.8% R)	−4 −56 22	0.083	2.2920986E^{-19}	8.92
2	Inferior parietal lobule, angular gyrus	Left (100% L)	−48 −66 34	0.081	9.648886E^{-19}	8.76
3	Medial frontal pole	Bilateral (55.5% L; 44.5% R)	8 42 −6	0.050	3.8794934E^{-10}	6.15
4	Parahippocampal gyrus, hippocampus, amygdala	Right (100% R)	28 −14 −20	0.050	2.5647295E^{-10}	6.22
5	Inferior parietal lobule, angular gyrus	Right (100% R)	52 −60 34	0.062	2.4539084E^{-13}	7.23
6	Parahippocampal gyrus, hippocampus, amygdala	Left (100% L)	−28 −24 −12	0.048	1.2546583E^{-9}	5.96
7	Thalamus	Bilateral (62.8% L; 37.2% R)	−2 −12 6	0.051	2.144407E^{-10}	6.24
8	Crus I/II of the cerebellum (pyramis, inferior semilunar lobule and uvula)	Right (100% R)	30 −78 −34	0.037	3.5167733E^{-7}	4.96
9	Lobule and vermis IX of the cerebellum	Bilateral (76.7% L; 23.3% R)	−6 −56 −46	0.040	7.92126E^{-8}	5.24
10	Ventromedial prefrontal cortex, anterior cingulate cortex	Bilateral (87.9% L; 12.1% R)	0 50 32	0.042	2.4101716E^{-8}	5.46

ALE, activation likelihood estimation; dlPFC, dorsal lateral prefrontal cortex; L, left; MNI, Montreal Neurological Institute; R, right; SMA, supplementary motor area.

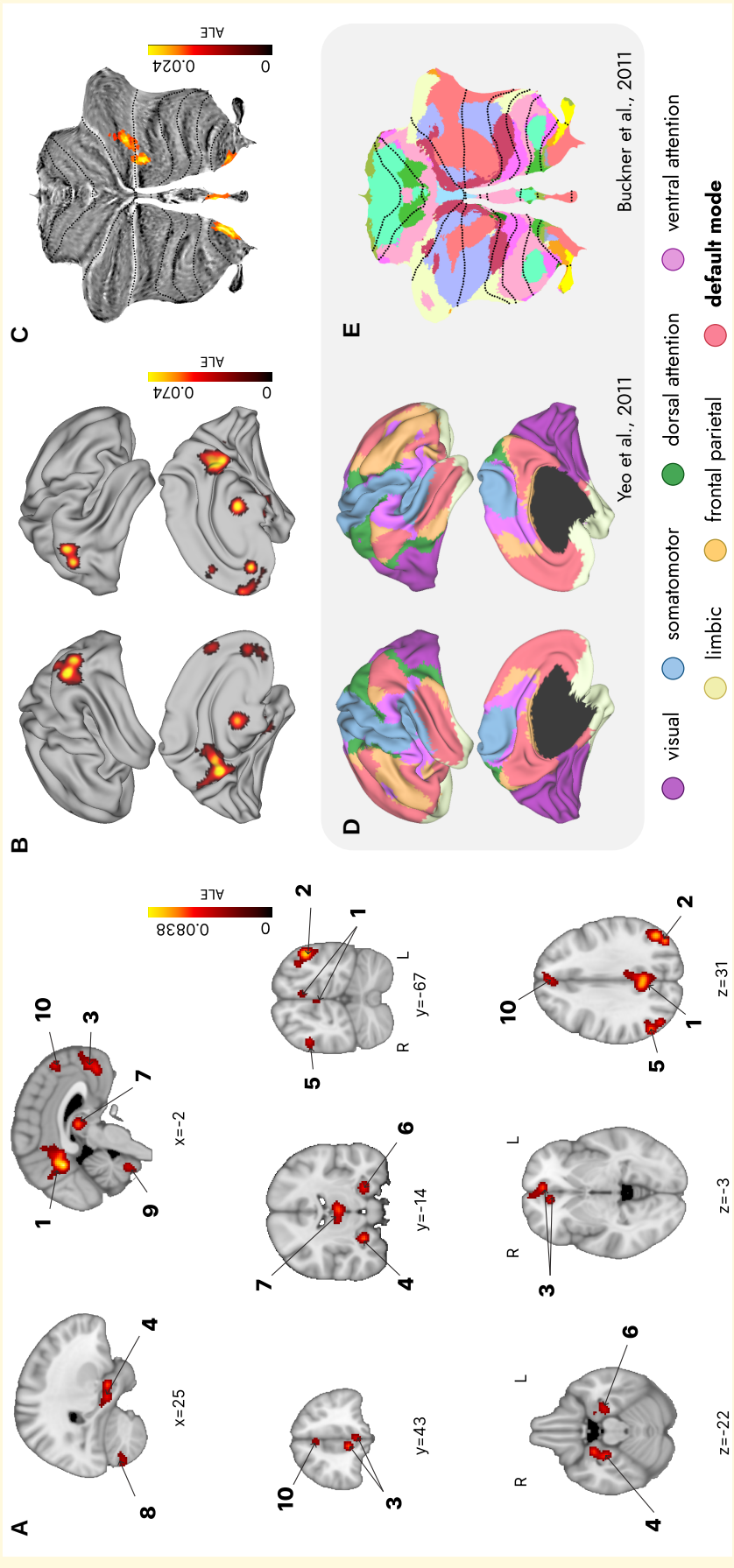

Figure 2 Cortical and subcortical brain regions of the default mode network. (**A**) The left panel displays the 10 spotted cortical and subcortical clusters of the resting-state default mode network on the standard MNI152 volume, determined by ALE meta-analysis with a cluster-level FWE correction of $P < 0.01$ (1000 permutations) and a cluster-forming threshold of $P < 0.001$. The same clusters are projected to a cortical surface (**B**) and to a cerebellar flatmap (**C**) for comparison with the default mode network represented on panels **D** and **E**. In panel **D**, the Yeo *et al.*[14] 7 resting-state network parcellation is displayed on a cortical surface, and in panel **E**, the cerebellar network parcellation by Buckner *et al.*[86] is displayed on a cerebellar flatmap.[72]

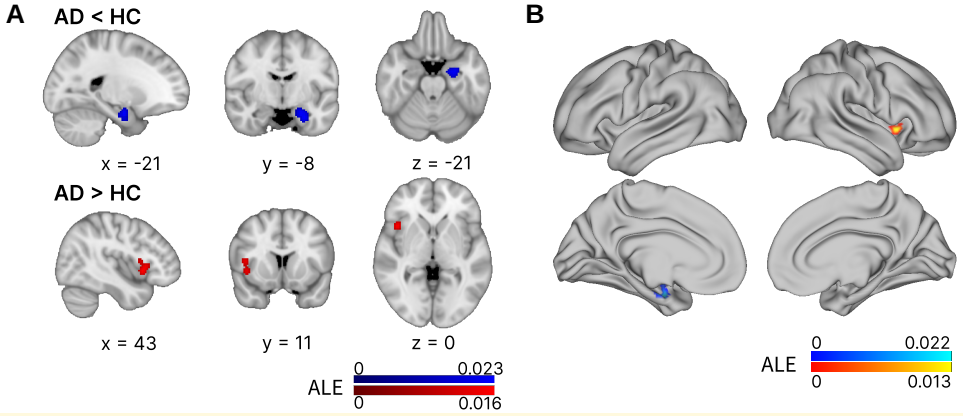

Figure 3 Brain sites of functional connectivity alterations in Alzheimer's disease. (**A**) This figure shows a volume view in standard MNI space of the ALE clusters with increased and decreased functional connectivity in Alzheimer's disease. The cluster in red indicates increases in Alzheimer's disease against controls, and the cluster in blue indicates decreases. In **B**, the same clusters are projected to the average surface for comparison with the resting-state networks displayed in Fig. 1A. These clusters were identified through ALE meta-analysis with a cluster-level FWE correction of $P < 0.05$ (1000 permutations) and a cluster-forming threshold of $P < 0.001$.

0.023; P-value = 8.412384E^{-7}; z-value = 4.79). The cluster of increased coactivation was 100% right-lateralized and covered the anterior insula and some of the precentral gyrus, with a maximum ALE value of 0.0164 at 42, 14 and −2 MNI coordinates (P-value = 3.911245E^{-6}; z-value = 4.47).

Empirical validation of the default mode network clusters

The group map of functional connectivity to all ROIs displayed coactivation with precuneus, posterior cingulate cortex, ventromedial prefrontal cortex, frontal pole, orbitofrontal cortex, anterior insula, inferior parietal cortex, precentral and postcentral gyri, hippocampus, left middle temporal gyrus, left fusiform gyrus, bilateral Crus I/II and in lobule IX of the cerebellum, mediodorsal and pulvinar nuclei of the thalamus, caudate nucleus, amygdala and basal forebrain (see Fig. 4A and Supplementary Table 6). Each meta-analytical seed showed significant functional connectivity to the other default mode network brain regions (see Supplementary Figs. 2 and 3 and Supplementary Tables 7–17). The conjunction analysis of functional connectivity maps of meta-analytical ROIs showed that all seeds connected to the precuneus, posterior cingulate cortex, ventromedial prefrontal cortex, frontal pole, inferior parietal cortex, hippocampus, left middle temporal gyrus and small clusters in the parahippocampal cortex, bilateral Crus I/II and in lobule IX of the cerebellum, anterior insula, basal forebrain and in the pulvinar nuclei of the thalamus (see Fig. 4B; refer to Supplementary Fig. 4 for additional results obtained using less stringent statistical thresholds).

Networks of the brain sites of functional connectivity alterations in Alzheimer's disease

The seed-based functional connectivity analysis of the decreased functional connectivity site in Alzheimer's disease showed connectivity to the precuneus cortex, posterior cingulate cortex, ventromedial prefrontal cortex, precentral and postcentral gyri, bilateral hippocampi, amygdala, parahippocampal gyri, superior and middle temporal gyri, temporal pole, inferior parietal cortex, basal forebrain, Crus I/II and lobule IX of the cerebellum and fusiform cortex (see Fig. 5A). The increased functional connectivity site displayed connectivity to the cuneus; intracalcarine and supracalcarine cortex; lingual gyrus; occipital pole; insula; opercular cortex; inferior parietal lobule; intraparietal sulcus; anterior and posterior cingulate cortices; supplementary motor cortex; precentral and postcentral gyri; ventromedial, orbitofrontal and dorsolateral prefrontal cortices; triangularis and opercularis; lobules V, VI, VIIb, VIIIa, IX and Crus II of the cerebellum; putamen; and middle thalamus (see Fig. 5B; see also Supplementary Figs. 5 and 6 for results obtained using less stringent statistical thresholds).

Conjunction analysis of default mode network and Alzheimer's disease alterations

Given the meta-analytical clusters for the default mode network and the functional connectivity alteration in Alzheimer's disease, we observed an overlap between the default mode network's cluster 6 and the Alzheimer's disease cluster of decreased functional connectivity. To extract the common cluster of voxels between these two clusters, we

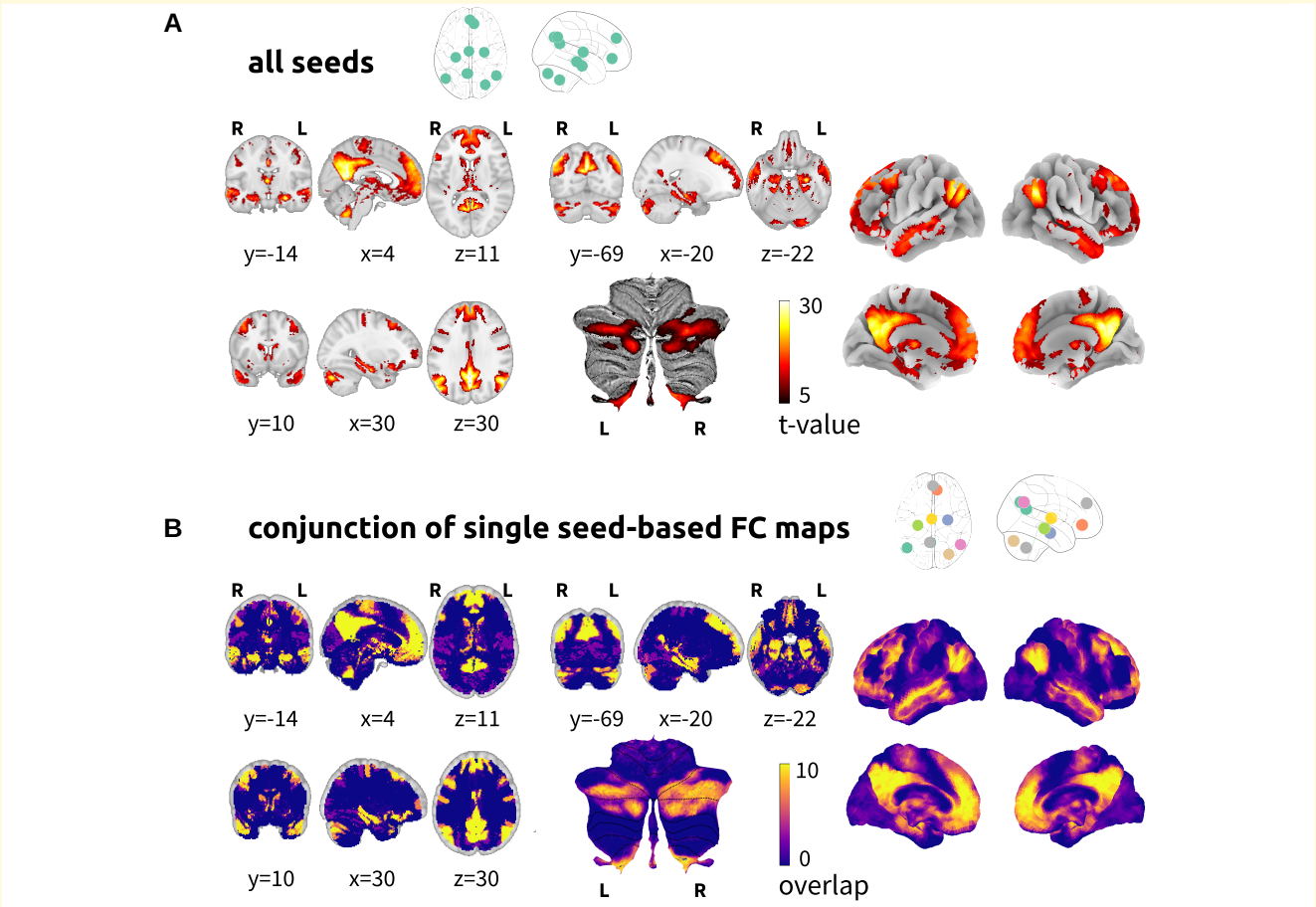

Figure 4 Validation analysis of the default mode network in the HCP 7T data set. (**A**) A group functional connectivity map is displayed in panel **A** for the functional connectivity map to the mask containing all clusters (voxel-wise 1-sample *t*-tests with 5000 permutations and threshold-free cluster enhancement at $P < 0.001$). (**B**) Results from the conjunction analysis of the functional connectivity maps from each seeded cluster (see also Supplementary Figs. 5 and 6).

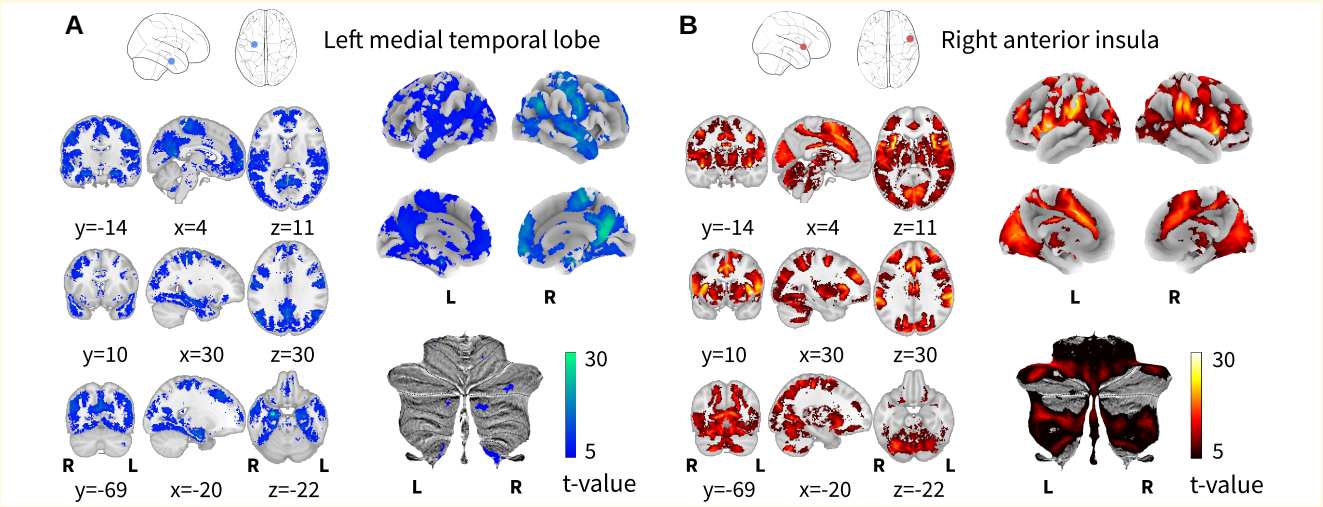

Figure 5 ROI-to-network analysis of Alzheimer's disease–altered brain sites. (**A**) Functional connectivity map from the ALE meta-analysis cluster of decreased functional connectivity. (**B**) Functional connectivity map from the meta-analysis cluster of increased connectivity. Both maps were calculated with a voxel-wise 1-sample *t*-tests with 5000 permutations and threshold-free cluster enhancement at $P < 0.001$.

thresholded the volumes with ALE values of the default mode network meta-analysis and the meta-analysis of decreased functional connectivity in Alzheimer's disease at ALE = 0.015 and performed a conjunction analysis, again using the AFNI function `3dcalc`. The resulting overlapping cluster consisted of 902 629 voxels that covered the left anterior hippocampus and left amygdala around MNI coordinates −22, −9 and −21.

Discussion

The default mode network has been extensively studied in the cortex and increasingly studied in the subcortex. However, there still is a lack of consensus on the specific subcortical regions involved in the default mode network and their functional connectivity changes in Alzheimer's disease. Our study combined systematic review, meta-analysis, empirical validation and network analysis to examine the brain regions conforming the default mode network in healthy adults and those showing altered functional connectivity in Alzheimer's disease. We identified and validated 10 clusters within the default mode network of healthy adults (5 subcortical clusters). We also found a consistent decrease in functional connectivity in the left anterior hippocampus and left amygdala overlapping with the subcortical default mode network. These findings expand our understanding of the default mode network and its relevance to Alzheimer's disease.

Among the 10 clusters identified in the default mode network, 7 were located in regions typically associated with the cortical components of the default mode network. These include the precuneus, posterior cingulate cortex, inferior parietal lobule, angular gyrus, ventromedial prefrontal and anterior cingulate cortices, medial frontal pole and medial temporal lobe, including the hippocampus.[73] These regions primarily constitute the medial temporal lobe and core subsystems of the default mode network, involved in mnemonic scene construction (i.e. in building mental scenes from memory).[16] Our validation analysis identified functional connectivity between these default mode network regions and other cortical default mode network regions, specifically the middle and superior temporal gyri and the dorsal prefrontal cortex,[73] potentially covering the entire cortical default mode network.

Our results extend beyond well-known cortical brain regions, revealing the consistent inclusion of subcortical brain regions in the default mode network. The thalamus, amygdala and specific areas of the cerebellum—Crus I/II and lobule and vermis IX—were present, which is consistent with previous results. The thalamus has been identified in multiple previous studies.[20,21,74-80] Our meta-analysis specifically highlights a middle and medial cluster covering the mediodorsal nucleus, and our validation analysis points to a medial and posterior thalamic cluster covering the pulvinar complex. Previous studies find functional connectivity between the default mode network and the anterior mediodorsal thalamus,[20] the central lateral nucleus,[21] the paraventricular thalamus[76,78] and to an anterior portion of the right and a posterior portion of the left thalamus.[81] Considering this variability and the resolution of the results from this meta-analysis, the specific contributions within the thalamus remain unclear. Brain areas within the cortical default mode network also coactivate with the amygdala[29,82-84] (with laterobasal, superficial and centromedial nuclei) and the cerebellum (CrusI/II and lobule and vermis IX, with some reports on lobules VIIIB and X).[30,76,85-87]

We identified five consistent subcortical brain regions of the default mode network, acknowledging that other subcortical regions might contribute but remain undetected. Although most studies show cerebellar contributions to the default mode network from the Crus I/II and lobule IX,[76,86,87] some studies point to vermis X, lobule VIIIB or the dentate gyrus nucleus.[76,87,88] Also, some previous studies had found functional connectivity with the basal forebrain, the caudate nucleus, the nucleus accumbens and the ventral tegmental area.[20,21] Also, despite incorporating numerous coordinates from the brainstem in our meta-analyses, the lack of sufficient overlap and consistency among studies, together with the application of stringent thresholds (see Supplementary Fig. 4), possibly prevented the identification of a meta-analytical cluster in this region.

The default mode network regions presented herein are anatomically connected[89-91] through the cingulum anterior and posterior tracts, the superior and inferior longitudinal fascicles, the arcuate fasciculus, the uncinate fasciculus, the frontal orbitopolar fasciculus and the corpus callosum.[4,20,30,89,92] Research using diffusion tensor imaging tractography has identified tracts that connect default mode network regions to the thalamus and basal forebrain.[20] The thalamus is connected to the cortical default mode network by the anterior thalamic radiations, the basal forebrain by the cingulum and fornix, and the thalamus and basal forebrain are connected to each other by the bundle of Vicq D'Azyr. Other diffusion tensor imaging tractography studies define multiple tracts connecting the cerebellum to all brain lobes, including a dentate-pontine-cerebellar tract.[93] Viral tracing techniques show connections between Crus I and II and the prefrontal cortex ,[94] and the amygdala also has anatomical projections to the adjacent hippocampus and prefrontal cortex from its basolateral complex.[95,96]

The anatomical connections between the cortical and subcortical structures of the default mode network suggest its overlap with the Papez circuit, an anatomical network linked to emotion in 1937.[20,97-99] Key regions like the thalamus, posterior cingulate cortex and hippocampal formation are part of this circuit.[97] Subsequent research on this circuit made it evolve into a more complex network that is relevant for several neurological conditions, such as Alzheimer's disease.[12,98] For instance, deep brain stimulation targeting the Papez circuit has shown benefits in overall cognitive performance in Alzheimer's disease.[12] Additional structures and tracts have been incorporated into the Papez circuit

based on their anatomical connections, including the amygdala and Crus I and II.[100,101]

Default mode network regions display altered functional connectivity in Alzheimer's disease,[35,36] but the connection between the subcortical default mode network and Alzheimer's disease remains unclear. Our study identified a cluster of reduced functional connectivity in the left hippocampus, amygdala and parahippocampal gyrus, as well as the connectivity and convergence of this cluster with the default mode network. This finding resonates with previous findings of reduced functional connectivity in the default mode network in Alzheimer's disease,[48] and particularly a left-sided alteration in its posterior subnetwork,[102] and with findings of the connectivity between these medial temporal lobe regions and the default mode network[29,82-84,103] (with exceptions[104]). These findings mirror broader pathology associations with the cortical default mode network[40,105] and also align with a recently proposed model of Alzheimer's disease.[39] This model posits a bidirectional relationship between connectivity disruptions within the default mode network and the accumulation of protein pathologies, such as amyloid-beta and tau, with a crucial role of the medial temporal lobe in the intersection of pathologies.

Zooming into the amygdala, we note its multifaceted involvement in Alzheimer's disease. The amygdala is vulnerable to Alzheimer's disease pathologies, starting with neurofibrillary tangle pathology as early as in Braak and Braak phase II.[44,106] Alterations of the amygdala also extend to functional connectivity,[35,104,107] including a reduction in connectivity between left amygdala and default mode network regions.[108] This might be especially relevant, taking into account the role of the amygdala as one of various subcortical regions with a causal inhibitory role in the activity of the default mode network.[109] The left amygdala, as well as the hippocampus, presents volume reductions in Alzheimer's disease,[110] which are associated with the carriage of APOE-ϵ4 alleles.[111] Furthermore, there is an inverse relationship between tau brain accumulation and left amygdala shape.[112]

The relevance of the amygdala extends to its potential role in the spread of pathology within the medial temporal lobe. Traditional pathways, like the spread of neurofibrillary tangles from the entorhinal cortex to the posterior hippocampus, fail to account for early tangle presence in the anterior hippocampus.[113] The extensive anatomical and functional connections between the amygdala and anterior hippocampus and other early pathology sites, such as the locus coeruleus, transentorhinal cortex, the subiculum and Cornu Ammonis 1 (CA1), position the amygdala as a hypothesized alternative route for tangle propagation.[113-116] Our results, alongside referenced studies, suggest that reduced connectivity in the left amygdala and left hippocampus might constitute a neurobiological feature of Alzheimer's disease and could be a potential biomarker of the disease.[13] Future studies should explore how the connectivity between the hippocampal/amygdalar cluster and the default mode network correlates with protein aggregation in these areas.

We also identified increased functional connectivity in the right anterior insula, as well as the connectivity of this cluster to a mixture of visual, ventral attention or salience networks' areas in an ultrahigh magnetic field sample of healthy young adults. Among the often overlapping salience and ventral attention networks, the former is bilateral, while the latter is right-lateralized.[117,118] These networks show increased functional connectivity in Alzheimer's disease,[119-124] associated with preserved or improved social cognition, as well as with irritability and signs of anxiety.[124,125] The anterior insula is also involved in a system for conscious access to sensory information,[126] and volume loss and fluorodeoxyglucose (FDG)-PET hypometabolism of the right anterior insula is associated with hallucinations in Alzheimer's disease.[127] Furthermore, the anterior insula, along with the locus coeruleus, mediodorsal thalamus and basal forebrain,[27,32,126] is crucial for transitioning between the default mode network and networks related to external attention and executive control.[126]

We found consistent alteration of brain regions within the default mode and ventral attention networks. These networks compose a proposed brain system for allostasis (i.e. the process of regulating physiological functions to maintain homeostasis), with the amygdala and insula partially overlapping in both component networks.[128-130] In a speculative context, the overlapping regions could be linked to the finding of increased functional connectivity in default mode subnetworks.[49,50] In the context of Alzheimer's disease, there is a hypothesis suggesting allostatic overload, marked by chronic activation of stress pathways.[131,132] This chronic activation leads to insulin resistance, associated with Alzheimer's disease neuropathology, brain function and cognition (particularly, with cognitive aspects linked to the default mode and ventral attention networks, such as memory consolidation[133,134]). Insulin receptors, involved in these processes, are present in multiple brain regions including the hippocampus, amygdala and insula.[131,135]

Our findings indicate functional connectivity alterations in Alzheimer's disease primarily in the medial temporal lobe, diverging from some previous studies that also report changes in cortical areas like the precuneus and ventromedial prefrontal cortex, and in early-affected regions like the thalamus and locus coeruleus.[34-36,48,54,136] The absence of identified alterations in subcortical default mode network structures other than the amygdala could be due to a lack of shared data; small sample sizes of some studies; heterogeneous patient groups potentially due to, for example, age differences among studies[137]; or other methodological issues. To gain a clearer understanding of these issues, we recommend future original research studies involving higher-resolution data and larger sample sizes. Notwithstanding these discrepancies, our functional connectivity map for the medial temporal lobe cluster aligns well with the spatial pattern of the default mode network.

The samples of Alzheimer's disease patients in the included experiments primarily consisted of individuals that typically exhibit noticeable cognitive decline but still retain

a degree of independence in daily activities (CDR scores 0.5–1.3).[138] These individuals average around 12 years of education, often corresponding to high school completion. Depending on the country of origin, this level of education might contribute to cognitive reserve, potentially enhancing compensatory mechanisms reflected in the increased connectivity of the insula.[139] Such compensatory mechanisms could serve to maintain cognitive function amidst aging and disease onset, as suggested by the Compensation-Related Utilization of Neural Circuits Hypothesis (CRUNCH) and Scaffolding Theory of Aging and Cognition (STAC) models.[140,141] Alternatively, the increased connectivity of the insula may rather directly stem from the initial pathology.[142,143] It is also noteworthy that we included studies that did not report Alzheimer's disease subtypes (e.g. hippocampal sparing). This suggests a more homogenous disease profile.

A potential limitation of this study is that the data are constrained by the availability of coordinates or brain maps in previous research, potentially biasing results towards more commonly reported regions. Coordinates are more often available than whole-brain statistical maps which lead to lower spatial resolution in the data and meta-analysis results, as well as to variability in criteria used to extract coordinates (e.g. amount of peak coordinates per cluster and centre of mass). This makes it difficult to, for example, discern between nuclei of subcortical regions. To address this issue, it is important to promote open research, including the use of open repositories for neuroimaging data such as NeuroVault, openfMRI and OpenNeuro.[62,144,145] Another limitation is the presence of relatively small sample sizes of about 20 subjects in some studies.[20] Future studies should also design appropriate ways in which to take into account the differential power of brain regions in functional connectivity.[146] Methodological limitations in previous studies might also explain why certain subcortical regions are missing from our findings and existing literature. Despite exclusively including studies of all brain regions, with volume- or combined volume- and surface-based analysis approaches, factors like those outlined in our introduction could lead to an underrepresentation of the subcortical the default mode network.[17] This includes challenges like extracting functional connectivity using signals with low signal-to-noise ratios in subcortical structures and difficulties in aligning small, variable subcortical regions for group analysis.[20,24,59,60]

This study has advanced our understanding of the subcortical structures that make up the default mode network and its alteration in Alzheimer's disease. This study has also identified both cortical and subcortical brain regions that exhibit functional connectivity changes in Alzheimer's disease, as well as the direction of the changes and their connection to whole-brain intrinsic functional connectivity. The participation of small subcortical regions and subparts of subcortical regions, as well as the extent of alterations in the subcortical default mode network in Alzheimer's disease, remains unclear. Further research is needed, for example, expanding our seed-based connectivity analysis to Alzheimer's disease patients and age-matched controls. It is also important to continue promoting open research practices in order to improve the coverage and unbiased approach of meta-analytical studies.

Supplementary material

Supplementary material is available at *Brain Communications* online.

Funding

This study was supported by grants TESIS2019010146 and EST2022010045 from the Board of Economy, Industry, Trade and Knowledge of the Canarian Government with a European Social Fund co-financing rate to S.S. and PSI2017-84933-P and PSI2017-91955-EXP to N.J. M.v.d.H. is funded by a European Research Council consolidator grant (ID 101001062 CONNECT), and A.A. is funded by a Spanish Agencia Estatal de Investigacion grant (ref: AEI/10.13039/501100011033).

Competing interests

M.v.d.H works as a data analysis consultant for Roche and is part of the editorial board of Human Brain Mapping. All other authors report no competing interests.

Data availability

All brain maps derived from this study are publicly available at https://github.com/Sleosoz/subcortical-DMN-and-Alzheimer.

References

1. Ingvar DH. 'Hyperfrontal' distribution of the cerebral grey matter flow in resting wakefulness; on the functional anatomy of the conscious state. *Acta Neurol Scand*. 1979;60:12-25.
2. Shulman G, Fiez JA, Corbetta M, Buckner R, Meizin F, Raichle M. Common blood flow changes across visual tasks: II. Decreases in cerebral cortex. *J Cogn Neurosci*. 1997;9:648-663.
3. Greicius MD, Krasnow B, Reiss AL, Menon V. Functional connectivity in the resting brain: A network analysis of the default mode hypothesis. *Proc Natl Acad Sci USA*. 2003;100:253-258.
4. Horn A, Ostwald D, Reisert M, Blankenburg F. The structural–functional connectome and the default mode network of the human brain. *Neuroimage*. 2014;102:142-151.
5. Liu C, Yen CCC, Szczupak D, Ye FQ, Leopold DA, Silva AC. Anatomical and functional investigation of the marmoset default mode network. *Nat Commun*. 2019;10:1975.
6. Fox MD, Snyder AZ, Vincent JL, Corbetta M, Van Essen DC, Raichle ME. The human brain is intrinsically organized into dynamic, anticorrelated functional networks. *Proc Natl Acad Sci USA*. 2005;102:9673-9678.
7. Raichle ME, MacLeod AM, Snyder AZ, Powers WJ, Gusnard DA, Shulman GL. A default mode of brain function. *Proc Natl Acad Sci USA*. 2001;98:676-682.

8. Hare SM, Ford JM, Mathalon DH, *et al.* Salience–default mode functional network connectivity linked to positive and negative symptoms of Schizophrenia. *Schizophr Bull*. 2019;45:892-901.
9. Eijlers AJ, Meijer KA, Wassenaar TM, *et al.* Increased default-mode network centrality in cognitively impaired multiple sclerosis patients. *Neurology*. 2017;88:952-960.
10. Mevel K, Chételat G, Eustache F, Desgranges B. The default mode network in healthy aging and Alzheimer's disease. *Int J Alzheimers Dis*. 2011;2011:535816.
11. Pascoal TA, Mathotaarachchi S, Kang MS, *et al.* Aβ-induced vulnerability propagates via the brain's default mode network. *Nat Commun*. 2019;10:2353.
12. Ríos AS, Oxenford S, Neudorfer C, *et al.* Optimal deep brain stimulation sites and networks for stimulation of the fornix in Alzheimer's disease. *Nat Commun*. 2022;13:7707.
13. Sperling R. Potential of functional MRI as a biomarker in early Alzheimer's disease. *Neurobiol Aging*. 2011;32(Suppl 1):S37-S43.
14. Yeo BT, Krienen FM, Sepulcre J, *et al.* The organization of the human cerebral cortex estimated by intrinsic functional connectivity. *J Neurophysiol*. 2011;106:1125-1165.
15. Margulies DS, Ghosh SS, Goulas A, *et al.* Situating the default-mode network along a principal gradient of macroscale cortical organization. *Proc Natl Acad Sci USA*. 2016;113:12574-12579.
16. Andrews-Hanna JR, Reidler JS, Sepulcre J, Poulin R, Buckner RL. Functional-anatomic fractionation of the brain's default network. *Neuron*. 2010;65:550-562.
17. Smith SM, Fox PT, Miller KL, *et al.* Correspondence of the brain's functional architecture during activation and rest. *Proc Natl Acad Sci USA*. 2009;106:13040-13045.
18. Laird AR, Eickhoff SB, Li K, Robin DA, Glahn DC, Fox PT. Investigating the functional heterogeneity of the default mode network using coordinate-based meta-analytic modeling. *J Neurosci*. 2009;29:14496-14505.
19. Ji JL, Spronk M, Kulkarni K, Repovš G, Anticevic A, Cole MW. Mapping the human brain's cortical-subcortical functional network organization. *Neuroimage*. 2019;185:35-57.
20. Alves PN, Foulon C, Karolis V, *et al.* An improved neuroanatomical model of the default-mode network reconciles previous neuroimaging and neuropathological findings. *Commun Biol*. 2019;2:370.
21. Li J, Curley WH, Guerin B, *et al.* Mapping the subcortical connectivity of the human default mode network. *Neuroimage*. 2021;245:118758.
22. Choi EY, Yeo BTT, Buckner RL. The organization of the human striatum estimated by intrinsic functional connectivity. *J Neurophysiol*. 2012;108:2242-2263.
23. Lebrun-Grandié P, Baron JC, Soussaline F, Loch'h C, Sastre J, Bousser MG. Coupling between regional blood flow and oxygen utilization in the normal human brain. A study with positron tomography and oxygen 15. *Arch Neurol*. 1983;40:230-236.
24. Bastos AM, Schoffelen J-M. A tutorial review of functional connectivity analysis methods and their interpretational pitfalls. *Front Syst Neurosci*. 2016;9:175.
25. Kahn I, Andrews-Hanna JR, Vincent JL, Snyder AZ, Buckner RL. Distinct cortical anatomy linked to subregions of the medial temporal lobe revealed by intrinsic functional connectivity. *J Neurophysiol*. 2008;100:129-139.
26. Aguilar DD, McNally JM. Subcortical control of the default mode network: Role of the basal forebrain and implications for neuropsychiatric disorders. *Brain Res Bull*. 2022;185:129-139.
27. Harrison BJ, Davey CG, Savage HS, *et al.* Dynamic subcortical modulators of human default mode network function. *Cereb Cortex*. 2022;32:4345-4355.
28. Cunningham SI, Tomasi D, Volkow ND. Structural and functional connectivity of the precuneus and thalamus to the default mode network. *Hum Brain Mapp*. 2017;38:938-956.
29. Bzdok D, Laird AR, Zilles K, Fox PT, Eickhoff SB. An investigation of the structural, connectional, and functional subspecialization in the human amygdala. *Hum Brain Mapp*. 2013;34:3247-3266.
30. Habas C, Kamdar N, Nguyen D, *et al.* Distinct cerebellar contributions to intrinsic connectivity networks. *J Neurosci*. 2009;29:8586-8594.
31. Bär KJ, de la Cruz F, Schumann A, *et al.* Functional connectivity and network analysis of midbrain and brainstem nuclei. *Neuroimage*. 2016;134:53-63.
32. Munn BR, Müller EJ, Wainstein G, Shine JM. The ascending arousal system shapes neural dynamics to mediate awareness of cognitive states. *Nat Commun*. 2021;12:6016.
33. Braak H, Thal DR, Ghebremedhin E, Del Tredici K. Stages of the pathologic process in Alzheimer disease: Age categories from 1 to 100 years. *J Neuropathol Exp Neurol*. 2011;70:960-969.
34. Aggleton JP, Pralus A, Nelson AJD, Hornberger M. Thalamic pathology and memory loss in early Alzheimer's disease: Moving the focus from the medial temporal lobe to Papez circuit. *Brain*. 2016;139:1877-1890.
35. Yao H, Liu Y, Zhou B, *et al.* Decreased functional connectivity of the amygdala in Alzheimer's disease revealed by resting-state fMRI. *Eur J Radiol*. 2013;82:1531-1538.
36. Zhou B, Liu Y, Zhang Z, *et al.* Impaired functional connectivity of the thalamus in Alzheimer' s disease and mild cognitive impairment: A resting-state fMRI study. *Curr Alzheimer Res*. 2013;10:754-766.
37. Braak H, Del Tredici K. Neuroanatomy and pathology of sporadic Alzheimer's disease. *Adv Anat Embryol Cell Biol*. 2015;215:1-2.
38. Guzmán-Vélez E, Diez I, Schoemaker D, *et al.* Amyloid-β and tau pathologies relate to distinctive brain dysconnectomics in preclinical autosomal-dominant Alzheimer's disease. *Proc Natl Acad Sci USA*. 2022;119:e2113641119.
39. Pasquini L, Rahmani F, Maleki-Balajoo S, *et al.* Medial temporal lobe disconnection and hyperexcitability across Alzheimer's disease stages. *J Alzheimers Dis Rep*. 2019;3:103-112.
40. Buckner RL, Sepulcre J, Talukdar T, *et al.* Cortical hubs revealed by intrinsic functional connectivity: Mapping, assessment of stability, and relation to Alzheimer's disease. *J Neurosci*. 2009;29:1860-1873.
41. Thal DR, Rüb U, Orantes M, Braak H. Phases of A beta-deposition in the human brain and its relevance for the development of AD. *Neurology*. 2002;58:1791-1800.
42. Parvizi J, Van Hoesen GW, Damasio A. The selective vulnerability of brainstem nuclei to Alzheimer's disease. *Ann Neurol*. 2001;49:53-66.
43. Kromer Vogt LJ, Hyman BT, Van Hoesen GW, Damasio AR. Pathological alterations in the amygdala in Alzheimer's disease. *Neuroscience*. 1990;37:377-385.
44. Braak H, Braak E. Neuropathological stageing of Alzheimer-related changes. *Acta Neuropathol*. 1991;82:239-259.
45. Braak H, Braak E, Bohl J, Lang W. Alzheimer's disease: Amyloid plaques in the cerebellum. *J Neurol Sci*. 1989;93:277-287.
46. Nakabayashi J, Yoshimura M, Morishima-Kawashima M, *et al.* Amyloid beta-protein (A beta) accumulation in the putamen and mammillary body during aging and in Alzheimer disease. *J Neuropathol Exp Neurol*. 1998;57:343-352.
47. Yu M, Sporns O, Saykin AJ. The human connectome in Alzheimer disease—Relationship to biomarkers and genetics. *Nat Rev Neurol*. 2021;17:545-563.
48. Badhwar A, Tam A, Dansereau C, Orban P, Hoffstaedter F, Bellec P. Resting-state network dysfunction in Alzheimer's disease: A systematic review and meta-analysis. *Alzheimers Dement*. 2017;8:73-85.
49. Damoiseaux JS, Prater KE, Miller BL, Greicius MD. Functional connectivity tracks clinical deterioration in Alzheimer's disease. *Neurobiol Aging*. 2012;33:828.e19-828.e30.
50. Zhang HY, Wang SJ, Xing J, *et al.* Detection of PCC functional connectivity characteristics in resting-state fMRI in mild Alzheimer's disease. *Behav Brain Res*. 2009;197:103-108.
51. Xue J, Guo H, Gao Y, *et al.* Altered directed functional connectivity of the hippocampus in mild cognitive impairment and

Alzheimer's disease: A resting-state fMRI study. *Front Aging Neurosci*. 2019;11:326.
52. Allen G, Barnard H, McColl R, *et al*. Reduced hippocampal functional connectivity in Alzheimer disease. *Arch Neurol*. 2007;64: 1482-1487.
53. Westlye ET, Lundervold A, Rootwelt H, Lundervold AJ, Westlye LT. Increased hippocampal default mode synchronization during rest in middle-aged and elderly APOE ϵ4 carriers: Relationships with memory performance. *J Neurosci*. 2011;31:7775-7783.
54. Tang F, Zhu D. Differences changes in cerebellar functional connectivity between mild cognitive impairment and Alzheimer's disease: A seed-based approach. *Front Neurol*. 2021;12:645171.
55. Braak H, Braak E. Alzheimer's disease affects limbic nuclei of the thalamus. *Acta Neuropathol*. 1991;81:261-268.
56. Xie L, Wisse LE, Das SR, *et al*. Longitudinal atrophy in early Braak regions in preclinical Alzheimer's disease. *Hum Brain Mapp*. 2020; 41:4704-4717.
57. Coalson TS, Van Essen DC, Glasser MF. The impact of traditional neuroimaging methods on the spatial localization of cortical areas. *Proc Natl Acad Sci*. 2018;115:E6356-E6365.
58. Greicius MD, Srivastava G, Reiss AL, Menon V. Default-mode network activity distinguishes Alzheimer's disease from healthy aging: Evidence from functional MRI. *Proc Natl Acad Sci USA*. 2004;101:4637-4642.
59. Weiskopf N, Hutton C, Josephs O, Deichmann R. Optimal EPI parameters for reduction of susceptibility-induced BOLD sensitivity losses: A whole-brain analysis at 3 T and 1.5 T. *Neuroimage*. 2006;33:493-504.
60. Seoane S, Modroño C, González-Mora JL, Janssen N. Medial temporal lobe contributions to resting-state networks. *Brain Struct Funct*. 2022;227:995-1012.
61. Page MJ, Moher D, Bossuyt PM, *et al*. PRISMA 2020 explanation and elaboration: Updated guidance and exemplars for reporting systematic reviews. *BMJ*. 2021;372:n160.
62. Gorgolewski KJ, Varoquaux G, Rivera G, *et al*. NeuroVault.org: A web-based repository for collecting and sharing unthresholded statistical maps of the human brain. *Front Neuroinform*. 2015;9:8.
63. Brice R. *Critical Appraisal Skills Programme*. CASP CHECKLISTSCASP Retrieved.
64. Turkeltaub PE, Eden GF, Jones KM, Zeffiro TA. Meta-analysis of the functional neuroanatomy of single-word reading: Method and validation. *Neuroimage*. 2002;16:765-780.
65. Laird AR, Fox PM, Price CJ, *et al*. ALE meta-analysis: Controlling the false discovery rate and performing statistical contrasts. *Hum Brain Mapp*. 2005;25:155-164.
66. Samartsidis P, Montagna S, Nichols TE, Johnson TD. The coordinate-based meta-analysis of neuroimaging data. *Stat Sci*. 2017;32:580-599.
67. Turkeltaub PE, Eickhoff SB, Laird AR, Fox M, Wiener M, Fox P. Minimizing within-experiment and within-group effects in activation likelihood estimation meta-analyses. *Hum Brain Mapp*. 2012; 33:1-13.
68. Eickhoff SB, Laird AR, Grefkes C, Wang LE., Zilles K, Fox PT. Coordinate-based activation likelihood estimation meta-analysis of neuroimaging data: A random-effects approach based on empirical estimates of spatial uncertainty. *Hum Brain Mapp*. 2009;30: 2907-2926.
69. Van Essen DC, Ugurbil K, Auerbach E, *et al*. The Human Connectome Project: A data acquisition perspective. *Neuroimage*. 2012;62:2222-2231.
70. McKhann G, Drachman D, Folstein M, Katzman R, Price D, Stadlan EM. Clinical diagnosis of Alzheimer's disease: Report of the NINCDS-ADRDA Work Group under the auspices of Department of Health and Human Services Task Force on Alzheimer's Disease. *Neurology*. 1984;34:939-944.
71. McKhann GM, Knopman DS, Chertkow H, *et al*. The diagnosis of dementia due to Alzheimer's disease: Recommendations from the National Institute on Aging-Alzheimer's Association workgroups on diagnostic guidelines for Alzheimer's disease. *Alzheimers Dement*. 2011;7:263-269.
72. Diedrichsen J, Zotow E. Surface-based display of volume-averaged cerebellar imaging data. *PLoS ONE*. 2015;10:e0133402.
73. Raichle ME. The brain's default mode network. *Annu Rev Neurosci*. 2015;38:433-447.
74. Chase HW, Grace AA, Fox PT, Phillips ML, Eickhoff SB. Functional differentiation in the human ventromedial frontal lobe: A data-driven parcellation. *Hum Brain Mapp*. 2020;41: 3266-3283.
75. Grigg O, Grady CL. The default network and processing of personally relevant information: Converging evidence from task-related modulations and functional connectivity. *Neuropsychologia*. 2010;48:3815-3823.
76. Blessing EM, Beissner F, Schumann A, Brünner F, Bär K-J. A data-driven approach to mapping cortical and subcortical intrinsic functional connectivity along the longitudinal hippocampal axis. *Hum Brain Mapp*. 2016;37:462-476.
77. Lee T-W, Xue S-W. Functional connectivity maps based on hippocampal and thalamic dynamics may account for the default-mode network. *Eur J Neurosci*. 2018;47:388-398.
78. Kark SM, Birnie MT, Baram TZ, Yassa MA. Functional connectivity of the human paraventricular thalamic nucleus: Insights from high field functional MRI. *Front Integr Neurosci*. 2021;15: 662293.
79. Tsai PJ, Chen SCJ, Hsu CY, *et al*. Local awakening: Regional reorganizations of brain oscillations after sleep. *Neuroimage*. 2014; 102(Pt 2):894-903.
80. Bernard JA, Seidler RD, Hassevoort KM, *et al*. Resting state cortico-cerebellar functional connectivity networks: A comparison of anatomical and self-organizing map approaches. *Front Neuroanat*. 2012;6:31.
81. Kumar VJ, van Oort E, Scheffler K, Beckmann CF, Grodd W. Functional anatomy of the human thalamus at rest. *Neuroimage*. 2017;147:678-691.
82. Elvira UKA, Seoane S, Janssen J, Janssen N. Contributions of human amygdala nuclei to resting-state networks. *PLoS ONE*. 2022; 17:e0278962.
83. Kerestes R, Chase HW, Phillips ML, Ladouceur CD, Eickhoff SB. Multimodal evaluation of the amygdala's functional connectivity. *Neuroimage*. 2017;148:219-229.
84. Sylvester CM, Yu Q, Srivastava AB, *et al*. Individual-specific functional connectivity of the amygdala: A substrate for precision psychiatry. *Proc Natl Acad Sci USA*. 2020;117:3808-3818.
85. Krienen FM, Buckner RL. Segregated fronto-cerebellar circuits revealed by intrinsic functional connectivity. *Cereb Cortex*. 2009; 19:2485-2497.
86. Buckner RL, Krienen FM, Castellanos A, Diaz JC, Yeo BTT. The organization of the human cerebellum estimated by intrinsic functional connectivity. *J Neurophysiol*. 2011;106:2322-2345.
87. Kawabata K, Bagarinao E, Watanabe H, *et al*. Functional connector hubs in the cerebellum. *Neuroimage*. 2022;257:119263.
88. Bernard JA, Peltier SJ, Benson BL, *et al*. Dissociable functional networks of the human dentate nucleus. *Cereb Cortex*. 2014;24: 2151-2159.
89. van den Heuvel M, Mandl R, Luigjes J, Hulshoff Pol H. Microstructural organization of the cingulum tract and the level of default mode functional connectivity. *J Neurosci*. 2008;28: 10844-10851.
90. Johnston JM, Vaishnavi SN, Smyth MD, *et al*. Loss of resting interhemispheric functional connectivity after complete section of the corpus callosum. *J Neurosci*. 2008;28:6453-6458.
91. Greicius MD, Supekar K, Menon V, Dougherty RF. Resting-state functional connectivity reflects structural connectivity in the default mode network. *Cereb Cortex*. 2009;19:72-78.
92. Teipel SJ, Bokde AL, Meindl T, *et al*. White matter microstructure underlying default mode network connectivity in the human brain. *Neuroimage*. 2010;49:2021-2032.

93. Karavasilis E, Christidi F, Velonakis G, *et al.* Ipsilateral and contralateral cerebro-cerebellar white matter connections: A diffusion tensor imaging study in healthy adults. *J Neuroradiol*. 2019;46:52-60.
94. Kelly RM, Strick PL. Cerebellar loops with motor cortex and prefrontal cortex of a nonhuman primate. *J Neurosci*. 2003;23:8432-8444.
95. Pikkarainen M, Rönkkö S, Savander V, Insausti R, Pitkänen A. Projections from the lateral, basal, and accessory basal nuclei of the amygdala to the hippocampal formation in rat. *J Comp Neurol*. 1999;403:229-260.
96. Petrovich GD, Canteras NS, Swanson LW. Combinatorial amygdalar inputs to hippocampal domains and hypothalamic behavior systems. *Brain Res Brain Res Rev*. 2001;38:247-289.
97. Papez JW. A proposed mechanism of emotion. *Arch NeurPsych*. 1937;38:725-743.
98. Marchesi O, Bonacchi R, Valsasina P, Rocca MA, Filippi M. Resting state effective connectivity abnormalities of the Papez circuit and cognitive performance in multiple sclerosis. *Mol Psychiatry*. 2022;27:3913-3919.
99. Wei PH, Mao ZQ, Cong F, *et al.* In vivo visualization of connections among revised Papez circuit hubs using full q-space diffusion spectrum imaging tractography. *Neuroscience*. 2017;357:400-410.
100. Choi S-H, Kim Y-B, Paek S-H, Cho Z-H. Papez circuit observed by in vivo human brain with 7.0T MRI super-resolution track density imaging and track tracing. *Front Neuroanat*. 2019;13:17.
101. Pisano TJ, Dhanerawala ZM, Kislin M, *et al.* Homologous organization of cerebellar pathways to sensory, motor, and associative forebrain. *Cell Rep*. 2021;36:109721.
102. Banks SJ, Zhuang X, Bayram E, *et al.* Default mode network lateralization and memory in healthy aging and Alzheimer's disease. *J Alzheimers Dis*. 2018;66:1223-1234.
103. Zidda F, Andoh J, Pohlack S, *et al.* Default mode network connectivity of fear- and anxiety-related cue and context conditioning. *Neuroimage*. 2018;165:190-199.
104. Ortner M, Pasquini L, Barat M, *et al.* Progressively disrupted intrinsic functional connectivity of basolateral amygdala in very early Alzheimer's disease. *Front Neurol*. 2016;7:132.
105. Schultz AP, Chhatwal JP, Hedden T, *et al.* Phases of hyperconnectivity and hypoconnectivity in the default mode and salience networks track with amyloid and tau in clinically normal individuals. *J Neurosci*. 2017;37:4323-4331.
106. Uchikado H, Lin W-L, DeLucia MW, Dickson DW. Alzheimer disease with amygdala Lewy bodies: A distinct form of α-synucleinopathy. *J Neuropathol Exp Neurol*. 2006;65:685-697.
107. Wang Z, Zhang M, Han Y, Song H, Guo R, Li K. Differentially disrupted functional connectivity of the subregions of the amygdala in Alzheimer's disease. *J X-ray Sci Technol*. 2016;24:329-342.
108. Du Y, Yu J, Liu M, *et al.* The relationship between depressive symptoms and cognitive function in Alzheimer's disease: The mediating effect of amygdala functional connectivity and radiomic features. *J Affect Disord*. 2023;330:101-109.
109. Zarghami TS. A new causal centrality measure reveals the prominent role of subcortical structures in the causal architecture of the extended default mode network. *Brain Struct Funct*. 2023;228:1917-1941.
110. He P, Qu H, Cai M, Liu W, Gu X, Ma Q. Structural alteration of medial temporal lobe subfield in the amnestic mild cognitive impairment stage of Alzheimer's disease. *Neural Plast*. 2022;2022:8461235.
111. Hobel Z, Isenberg AL, Raghupathy D, Mack W, Pa J, & Alzheimer's disease neuroimaging initiative. APOEε4 gene dose and sex effects on Alzheimer's disease MRI biomarkers in older adults with mild cognitive impairment. *J Alzheimers Dis*. 2019;71:647-658.
112. Lee YH, Bak Y, Park CH, *et al.* Patterns of olfactory functional networks in Parkinson's disease dementia and Alzheimer's dementia. *Neurobiol Aging*. 2020;89:63-70.
113. Stouffer KM, Grande X, Duezel E, *et al.* Amidst an amygdala renaissance in Alzheimer's disease. *Brain*. 2024;147:816-829.
114. Aggleton JP. A description of the amygdalo-hippocampal interconnections in the macaque monkey. *Exp Brain Res*. 1986;64:515-526.
115. Pitkänen A, Pikkarainen M, Nurminen N, Ylinen A. Reciprocal connections between the amygdala and the hippocampal formation, perirhinal cortex, and postrhinal cortex in rat. A review. *Ann N Y Acad Sci*. 2000;911:369-391.
116. Grande X, Sauvage MM, Becke A, Düzel E, Berron D. Transversal functional connectivity and scene-specific processing in the human entorhinal-hippocampal circuitry. *eLife*. 2022;11:e76479.
117. Corbetta M, Patel G, Shulman GL. The reorienting system of the human brain: From environment to theory of mind. *Neuron*. 2008;58:306-324.
118. Uddin LQ. Salience processing and insular cortical function and dysfunction. *Nat Rev Neurosci*. 2015;16:55-61.
119. Li H-J, Hou X-H, Liu H-H, Yue C-L, He Y, Zuo X-N. Toward systems neuroscience in mild cognitive impairment and Alzheimer's disease: A meta-analysis of 75 fMRI studies. *Hum Brain Mapp*. 2015;36:1217-1232.
120. Multani N, Taghdiri F, Anor CJ, Tang-Wai DF, Tartaglia MC. Association between social cognition changes and resting state functional connectivity in frontotemporal dementia, Alzheimer's disease, Parkinson's disease, and healthy controls. *Front Neurosci*. 2019;13:1259.
121. Altunkaya S, Huang SM, Hsu YH, *et al.* Dissociable functional brain networks associated with apathy in subcortical ischemic vascular disease and Alzheimer's disease. *Front Aging Neurosci*. 2022;13:717037.
122. Zhou J, Greicius MD, Gennatas ED, *et al.* Divergent network connectivity changes in behavioural variant frontotemporal dementia and Alzheimer's disease. *Brain*. 2010;133:1352-1367.
123. Gour N, Felician O, Didic M, *et al.* Functional connectivity changes differ in early and late-onset Alzheimer's disease. *Hum Brain Mapp*. 2014;35:2978-2994.
124. Seeley WW, Allman JM, Carlin DA, *et al.* Divergent social functioning in behavioral variant frontotemporal dementia and Alzheimer disease: Reciprocal networks and neuronal evolution. *Alzheimer Dis Assoc Disord*. 2007;21:S50-S57.
125. Zhou J, Seeley WW. Network dysfunction in Alzheimer's disease and frontotemporal dementia: Implications for psychiatry. *Biol Psychiatry*. 2014;75:565-573.
126. Huang Z, Tarnal V, Vlisides PE, *et al.* Anterior insula regulates brain network transitions that gate conscious access. *Cell Rep*. 2021;35:109081.
127. Blanc F, Noblet V, Philippi N, *et al.* Right anterior insula: Core region of hallucinations in cognitive neurodegenerative diseases. *PLoS ONE*. 2014;9:e114774.
128. Kleckner IR, Zhang J, Touroutoglou A, *et al.* Evidence for a large-scale brain system supporting allostasis and interoception in humans. *Nat Hum Behav*. 2017;1:0069.
129. Katsumi Y, Theriault JE, Quigley KS, Barrett LF. Allostasis as a core feature of hierarchical gradients in the human brain. *Netw Neurosci*. 2022;6:1010-1031.
130. Zhang J, Chen D, Srirangarajan T, *et al.* (2023) 'Cortical and subcortical mapping of the allostatic-interoceptive system in the human brain: Replication and extension with 7 Tesla fMRI', bioRxiv, https://doi.org/10.1101/2023.07.20.548178, 24 July 2023, preprint: not peer reviewed.
131. De Felice FG, Gonçalves RA, Ferreira ST. Impaired insulin signalling and allostatic load in Alzheimer disease. *Nat Rev Neurosci*. 2022;23:215-230.
132. Adedeji DO, Holleman J, Juster RP, *et al.* Longitudinal study of Alzheimer's disease biomarkers, allostatic load, and cognition among memory clinic patients. *Brain Behav Immun Health*. 2023;28:100592.
133. Lourenco MV, Clarke JR, Frozza RL, *et al.* TNF-α mediates PKR-dependent memory impairment and brain IRS-1 inhibition

induced by Alzheimer's β-amyloid oligomers in mice and monkeys. *Cell Metab*. 2013;18:831-843.
134. Soto M, Cai W, Konishi M, Kahn CR. Insulin signaling in the hippocampus and amygdala regulates metabolism and neurobehavior. *Proc Natl Acad Sci USA*. 2019;116:6379-6384.
135. Bolo NR, Musen G, Simonson DC, *et al.* Functional connectivity of insula, basal ganglia, and prefrontal executive control networks during hypoglycemia in type 1 diabetes. *J Neurosci*. 2015;35:11012-11023.
136. Almkvist O, Brüggen K, Nordberg A. Subcortical and cortical regions of amyloid-β pathology measured by 11C-PiB PET are differentially associated with cognitive functions and stages of disease in memory clinic patients. *J Alzheimers Dis*. 2021;81:1613-1624.
137. van de Mortel LA, Thomas RM, van Wingen GA, Alzheimer's Disease Neuroimaging Initiative. Grey matter loss at different stages of cognitive decline: A role for the thalamus in developing Alzheimer's disease. *J Alzheimers Dis*. 2021;83:705-720.
138. Morris JC. Clinical Dementia Rating: A reliable and valid diagnostic and staging measure for dementia of the Alzheimer type. *Int Psychogeriatr*. 1997;9(Suppl 1), 173-176; discussion 177–8.
139. Bozzali M, Dowling C, Serra L, *et al.* The impact of cognitive reserve on brain functional connectivity in Alzheimer's disease. *J Alzheimers Dis*. 2015;44:243-250.
140. Reuter-Lorenz PA, Cappell KA. Neurocognitive aging and the compensation hypothesis. *Curr Dir Psychol Sci*. 2008;17:177-182.
141. Reuter-Lorenz PA, Park DC. How does it STAC up? Revisiting the scaffolding theory of aging and cognition. *Neuropsychol Rev*. 2014;24:355-370.
142. Fredericks CA, Sturm VE, Brown JA, *et al.* Early affective changes and increased connectivity in preclinical Alzheimer's disease. *Alzheimers Dement*. 2018;10:471-479.
143. Xie C, Bai F, Yu H, *et al.* Abnormal insula functional network is associated with episodic memory decline in amnestic mild cognitive impairment. *Neuroimage*. 2012;63:320-327.
144. Poldrack RA, Barch DM, Mitchell JP, *et al.* Toward open sharing of task-based fMRI data: The OpenfMRI project. *Front Neuroinform*. 2013;7:12.
145. Markiewicz CJ, Gorgolewski KJ, Feingold F, *et al.* The OpenNeuro resource for sharing of neuroscience data. *eLife*. 2021;10:e71774.
146. Helwegen K, Libedinsky I, van den Heuvel MP. Statistical power in network neuroscience. *Trends Cogn Sci*. 2023;27:282-301.